IEEE Transactions on Transportation Electrification, Available online 28 March 2023
DOI: 10.1109/TTE.2023.3262208

More Electric Aircraft Conversion to All-Electric During Ground Operations: Battery-Powered Landing Gear Drive System

Jakub Deja[a] , Iman Dayyani[a], Varun Nair[a] and Martin Skote[a]

[a]School of Aerospace, Transport and Manufacturing, Cranfield University, MK43 0AL, Cranfield, UK

ARTICLE HISTORY
Published on 28th of March, 2023 in IEEE Transactions on Transportation Electrification.
DOI: 10.1109/TTE.2023.3262208

ABSTRACT
Raising awareness about environmental issues moves the aerospace industry towards electrification, and the corresponding solutions are already present at some airports. However, commercial aircraft are the missing links in claiming all-electric ground operations. They rely on fossil fuels without any electric alternative due to the technological inability to store large amounts of energy while maintaining a low weight of batteries. The issue diminishes if an electric system uses only a fraction of the energy normally consumed by the engines and comprises kinetic energy recovery. Accordingly, this article demonstrates the landing gear drive system for a narrowbody airplane, which has the sustainable and economic means to replace all onboard engines throughout ground operations. The system is simulated in MATLAB/Simulink and leads to the kinematic results that are based on the real drive cycles. The kinematics are subsequently used to estimate the overall on-ground power and energy demand of a more electric aircraft (MEA). The impact is maximized with the components scaled according to performance metrics and two-speed gear ratio optimization. The net fuel advantage is demonstrated for different ground operation modes, taxi times, and flight path lengths.

Index Terms: Aircraft, aircraft propulsion, energy recovery, energy storage.

CORRESPONDING AUTHOR: J. Deja. Email: jakub.deja@cranfield.ac.uk

Abbreviations

APU	Auxiliary power unit.
ECS	Environmental control system.
EGTS	Electric green taxi system.
ETOPS	Extended-range twin-engine operations performance standards.
ETS	Electric taxi system.
FOD	Foreign object damage.
ICE	Internal combustion engine.
KERS	Kinetic energy recovery system.
MEA	More electric aircraft.
SET	Single-engine taxi.

Nomenclature

ω_{em}	Angular velocity of electric machine.
ρ	Density of air.
A	Reference area for drag equation; A320 wing area.
C_d	Coefficient of drag.
C_{rr}	Coefficient of rolling resistance.
E_{dem}	Total energy demand of MEA for ground operations.
E_d	Energy transfer balance for drag.
E_{em}	Energy transfer balance for the landing gear drive system.
E_{met}	Energy transfer balance for main engines thrust.
E_{rr}	Energy transfer balance for rolling resistance.
E_{sds}	Energy transfer balance for the standard deceleration systems.
E	Energy transfer balance.
FC_{APU}	Average fuel consumption of auxiliary power unit per time unit.
FC_{me}	Average fuel consumption of single main engine per time unit.
FC_{pp}	In-flight fuel consumption per kilogram of payload-kilometer.
FP_{EGTS}	Fuel penalty incurred by electric green taxi and tug system ground operation mode.
FP_{oe}	Fuel penalty incurred by single-engine ground operation mode.
FP_{te}	Fuel penalty incurred by twin-engine ground operation mode.
FS_{EGTS}	Net fuel saving of landing gear drive system against electric green taxi and tug systems.

FS_{oe}	Net fuel saving of landing gear drive system against single-engine taxi.
FS_{te}	Net fuel saving of landing gear drive system against twin-engine taxi.
FU_{cd}	Fuel consumed during cooldown of main engines only.
FU_{iEGTS}	Fuel consumed during inbound electric green taxi or tug systems taxi.
FU_{ioe}	Fuel consumed during inbound single-engine taxi.
FU_{ite}	Fuel consumed during inbound twin-engine taxi.
FU_{oEGTS}	Fuel consumed during outbound electric green taxi or tug systems taxi.
FU_{ooe}	Fuel consumed during outbound single-engine taxi.
FU_{ote}	Fuel consumed during outbound twin-engine taxi.
FU_{toff}	Fuel saving during takeoff.
FU_{wup}	Fuel consumed during warmup of main engines only.
F_{d}	Force applied to longitudinal aircraft model due to drag.
F_{em}	Force applied to longitudinal aircraft model due to landing gear drive system.
F_{met}	Force applied to longitudinal aircraft model due to main engines thrust.
F_{rr}	Force applied to longitudinal aircraft model due to rolling resistance.
F_{sds}	Force applied to longitudinal aircraft model due to standard deceleration systems.
F	Force applied to longitudinal aircraft model.
KE_{ac}	Kinetic energy of aircraft longitudinal body.
K_{met}	Proportional gain of main engines thrust.
K_{pem}	Proportional gain of landing gear drive system controller.
K_{sds}	Proportional gain of standard deceleration systems controller.
P_{dem}	Peak power of landing gear drive system .
R_{txi}	Taxiing-in proportion to overall taxiing time.
R_{txo}	Taxiing-out proportion to overall taxiing time.
SE_{bat}	Specific energy of battery at given battery technology level.
SP_{dr}	Specific power of drivetrain at given technology level .
SP_{em}	Specific power of electric machines at given technology level .
SP_{pcon}	Specific power of power converter at given technology level.
S_{f}	Flight distance.
TSFC	Thrust specific fuel consumption for static conditions.
T_{em}	Torque produced by electric machine.
W_{APU}	Weight of auxiliary power unit and corresponding components.

W_{EGTS}	Weight of electric green taxi system and corresponding components.
W_{bat}	Total weight of battery of landing gear drive system.
W_{pow}	Total weight of powetrain and electric machines.
W_{tot}	Total weight of landing gear drive system.
f_{sat}	Function of electric machine saturation with respect to maximum torque and power.
g	gravitational acceleration, $9.81 m/s^2$.
i_{taxi}	Gear ratio for taxi.
i_{tl}	Gear ratio for takeoff and landing.
i	Gear ratio.
m_a	Mass of aircraft.
r_w	Wheel radius of main landing gear.
t_{CD}	Time length of main engines cooldown.
t_{ILAP}	Time length of overlap between auxiliary power unit and main engines in inbound phase.
t_{OLAP}	Time length of overlap between auxiliary power unit and main engines in outbound phase.
t_{PAR}	Time length of post-arrival.
t_{PD}	Time length of pre-departure.
t_{TXI}	Time length of taxi-in.
t_{TXO}	Time length of taxi-out.
t_{WUP}	Time length of main engines warmup.
t	Time.
v_a	Actual ground speed of aircraft in longitudinal frame.
v_{dem}	Aircraft ground speed demand set by drive cycle in longitudinal frame.

1. Introduction

The aviation industry is subjected to growth and the number of passenger aircraft in service is predicted to double by 2041 in comparison to the value from 2020 and accordingly, there are increasing concerns about greenhouse gas emissions [1]. Various bodies act to mitigate the harmful impacts and for example, European Union Aviation Safety Agency [2] prepared the Flightpath 2050 strategy which strives to limit the greenhouse gas and noise emissions. The aircraft manufacturers address the sustainable goals by developing a more fuel-efficient and environmentally friendly aircraft. This is being achieved with a more electric aircraft (MEA) where the systems that were originally powered by pneumatics and hydraulics are replaced with electric alternatives [3]. The ongoing electrification aligns well with the postulate of the Flightpath 2050 which requires the emission-free taxi movement by 2050 [2]. To meet this target, the widely used internal combustion engines (ICE) must be replaced including the auxiliary power unit (APU) which burns approximately 2 kg/min [4] of jet fuel and the main engines that burn 7.7 kg/min per engine [5] during ground movement of short-haul aircraft. Both ground and onboard systems have been proposed for replacing the ICE of aircraft, of which the most impactful are summarized below.

The improved ground operations of aircraft receive increasing attention and there are multiple publications that bring novelty to electric taxiing, APU removal, energy storage onboard commercial aircraft and gear aided takeoff. There are many electric taxi projects to date, including Safran's Electric Green Taxi System (EGTS), TaxiBot, WheelTug and the L-3's concepts [6]. There is also an outside-of-the-box idea that integrates both ground-fitted and onboard systems. Rohacs and Rohacs [7] led the GABRIEL project which uses a magnetic levitation ramp to electrically aid a takeoff and dissipate energy during landing. This ramp is combined with a separable tug device which is used for taxiing. Nevertheless, reliance on the ground-fitted deceleration systems without any backup led to safety concerns that must be addressed. Each of the systems listed above was brought to improve economy and sustainability of aircraft. The ground movement of aircraft with the main engines off leads to reduced noise and jet blast, making the ground handling personnel safer. Simultaneously, the overhaul cost of main engines per flight is reduced and the probability of unexpected foreign object damage (FOD) becomes smaller. The reduced brake wear rate occurs in contrast to the conventional ground movement where the main engines produce excessive thrust for taxi and therefore additional braking action is required. The unused brakes cool down much faster after a landing and therefore, a faster turnaround can be executed. These aspects together with the fuel savings lead to as much as 18% of mission cost reduction, which is equal to 1470 euro per standard European flight [7]. The list of advantages is longer for the onboard systems because reliance on the ground personnel and the tugs is reduced.

The onboard Electric Taxi Systems (ETS) to date source electric power from an APU because it consumes less fuel than main engines of aircraft during taxi. However, this approach requires a bespoke APU with higher electric power output. Lukic et al. [8] estimated that an 80-tonne single-aisle aircraft (Airbus A320 family size) requires as much as 240 kW, whereas the commonly fitted Honeywell 131-9A APU provides only 90 kW of electric output meaning that additional weight penalty associated with electric taxiing is expected. The recent developments in the ETS focus solely on power utilization of the system itself when, in fact, the all-electric ground operations require an energy storage that satisfies the power demand of multiple systems of an MEA. Pagonis [9] defined the electric loads for the key systems of a B787, including: (a) En-

vironmental control system (ECS) [352 kW], (b) hydraulics [40 kW], (c) flight controls [14 kW], (d) fuel pumps [32 kW] and (e) forward cargo air conditioning [60 kW]. A similar analysis was done by Wheeler et al. [10], who estimated that the power demand of the ECS equals 210 kW and the fuel pumps drain 10 kW. In addition, the author stated that operation of landing gear takes from 5 to 70 kW of power and the engine starters consume 200 kW. Herzog [11] approximated the electrical power consumption of the ECS for both a 100 passenger and a 350 passenger aircraft with the values reaching 90 and 400 kW respectively.

To fulfil the energy requirements, the suitable energy storage is needed and the best specific energy can be obtained with fuel cells. Stockford et al. [12] assessed the benefit and performance impact of the hydrogen powered fuel cells and claimed reduced weight in comparison to batteries. The primary downside of hydrogen and fuel cells is their lack of technological maturity which leads to tremendous but justified amount of objections coming from the aerospace bodies. In contrast, the Li-ion batteries are already present onboard the more-electric Boeing 787, though, their first years in service were badly eventful [13]. The present advancement of battery technology permits specific energy up to approximately 300 Wh/kg [14, 15].

The issue of low specific energy can be minimized by adding the kinetic energy recovery capability. Heinrich et al. [16] were the first to merge advantages of the kinetic energy recovery system (KERS) into the ETS, and investigated the regenerative braking capability during taxi for short-haul aircraft. They stated that KERS coupled to ETS can recover as much as 15% of energy required for taxi cycle. Their analysis excluded the possibility of energy recovery during a landing roll which would significantly increase the amount of harvested energy [17]. Nonetheless, the maximum charge rate of li-ion batteries is a limiting factor. At present, the battery can be charged up to 3 C [18] while recently the Li-Ion battery that sustains 6 C has been developed [19].

Combining these aspects together and adding the capability of regenerative braking during landing potentially allow to consider the battery powered ground operations with the landing gear drive system for a short-haul aircraft as sustainably and economically feasible. We propose a system that involves an energy storage onboard and therefore, an APU becomes redundant. Removal of this device and related components allows to save as much as 630 kg [20]. Furthermore, each aircraft has a Master Minimum Equipment List that defines what components and systems are critical for aircraft operation and the APU is unnecessary unless the flight is subjected to the Extended-range twin engine operations standards (ETOPS) where increased redundancy of the electric system becomes safety critical [21]. The main contributions of this paper are as follow: (1) Literature review to discuss the state-of-the-art of electric taxi and demonstrate the possibility for a battery powered version. (2) Demonstration of the battery-powered landing gear drive system and assessment of its impact on an Airbus A320 aircraft architecture. (3) Estimation of electric energy amount required to power the novel system together with the remaining MEA systems during ground operations. (4) Analysis of energy recovery capability during landing phase and taxiing. (5) Definition of the fuel savings equations and simulations to provide a comprehensive benchmark for all-electric ground operations against the conventional methods.

2. Landing Gear Drive System and Impact on Aircraft

A high-power landing gear drive system is demonstrated in this paper, which comprises the electric machines, the 4-quadrant power converters, the drivetrain and the

large-capacity energy storage. These components are more powerful than in the EGTS and allow an aircraft to accelerate faster, while the high-capacity battery allows to execute the ground operations without any ICE. In addition, the system aids the takeoff in parallel with the main engines. The landing gear drive system leads to further reduced noise and air pollution than the EGTS system, which sources power from the APU [22]. Figure 1 shows the system's demonstrator and the corresponding changes to the Airbus A320.

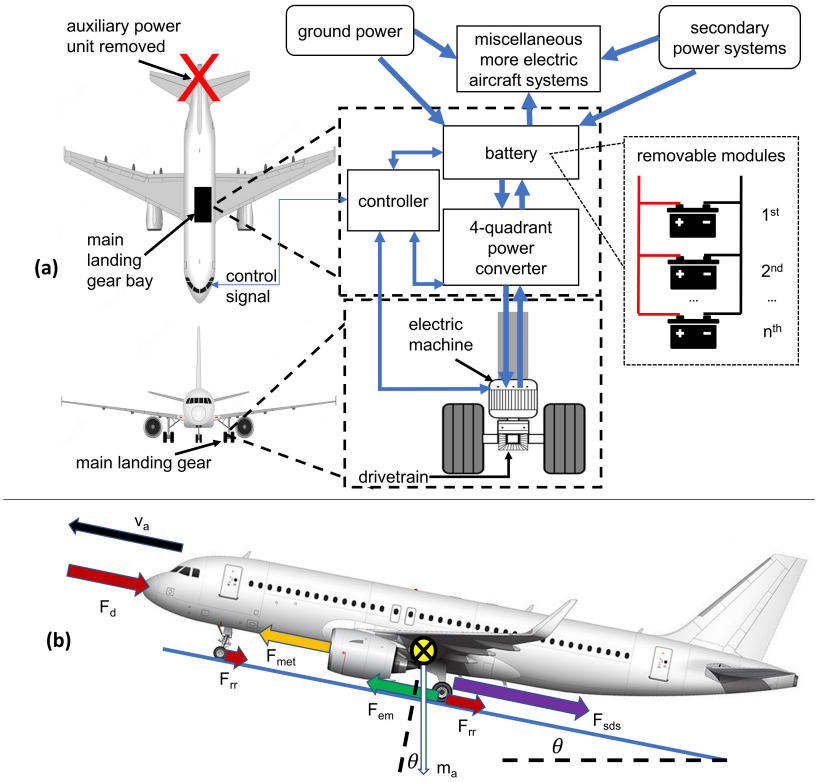

Figure 1. Demonstrator of the landing gear drive system. (a) System-level presentation among with impact on aircraft, (b) Free-body diagram of the aircraft.

Multiple modifications to the aircraft are required and primarily, the redesigned landing gear is needed to accommodate the large electric machine and the drivetrain. Figure 1 (a) shows the electric machine located in the main landing gear which is similar to Safran/Honeywell's EGTS [22]. Nevertheless, the landing gear drive system differs to any solution proposed to date with much higher torque and power and therefore, it takes more volume. The four-quadrant power converters are needed to control the electric machines during both propulsive and regenerative cycles. They are located in proximity to electric machines to minimize the wiring weight and to allow better heat exchange with ambient air. The controller is located in the electrical cabinet to ensure the safe operation environment for this electric device. To further increase safety, a pilot is capable of rapidly disengaging the system during any malfunction.

The battery pack is located in the fuselage and can be charged by either a ground power source or the main engines. If the battery depletes during ground operations, the aircraft can continue to taxi with the main engines. The battery is modular where each module is connected in parallel meaning that the ground crew can remove the

battery cells that are redundant for shorter taxi cycles. This design objective allows to reduce the weight and accordingly, maximize the fuel savings.

Another weight saving is achieved by completely removing the APU and corresponding components which leads to 265 kg of weight reduced [20]. In these circumstances, the battery can be considered as a back-up energy source for electrical systems during an ETOPS flight.

2.1. *Dynamic Model*

This section introduces the dynamic model which is created to determine the energy transfer during ground operations of an Airbus A320 equipped with the landing gear drive system. It is based on the free-body diagram shown in Figure 1 (b) and takes into account the following factors: (a) the landing gear drive system, (b) the standard deceleration systems, (c) thrust of main engines, (d) drag and (e) rolling resistance of aircraft. The incline of runway is only used to validate sufficiency of landing gear drive system torque during taxiing. Figure 2 shows in the block diagram the relationship between each subsystem and the influence of each factor on aircraft body.

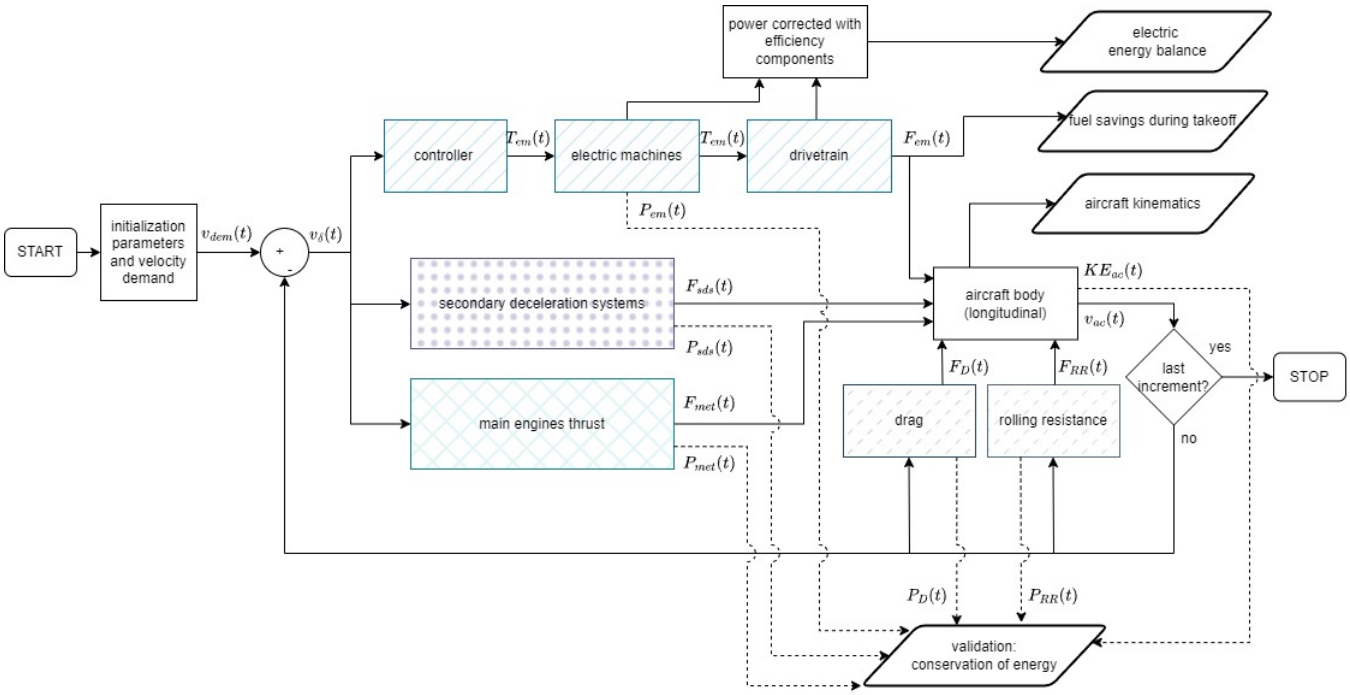

Figure 2. Dynamic model shown as block diagram disclosing the relation between multiple systems and the validation algorithm.

The longitudinal model of aircraft body is considered as a solid subjected to external forces $a = \frac{\sum F(t)}{m}$ and the lower order kinematics are obtained by integration with respect to time. The following forces are applied (all the variables are defined in the nomenclature and links are provided in an online version of this paper):

$$\sum F(t) = F_{em}(t) + F_{sds}(t) + F_{met}(t) + F_d(t) + F_{rr}(t) \tag{1}$$

where each factor is described as:

$$\begin{cases} F_{em}(t) = (v_{dem}(t) - v_a(t)) \times K_{pem} \times i(t) \times r_w \times 2 \\ F_{sds}(t) = (v_{dem}(t) - v_a(t)) \times K_{sds} \\ F_{met}(t) = (v_{dem}(t) - v_a(t)) \times K_{met} \\ F_d(t) = \frac{1}{2} {v_a}^2(t) \rho C_d A \\ F_{rr}(t) = C_{rr}(t) m_a g \end{cases} \tag{2}$$

and each system of aircraft has modelled saturation limits with the following saturation logic:

$$\begin{cases} v_{dem}(t) - v_a(t) \times K_{pem} \in (-f_{sat}(t), f_{sat}(t)) \text{ for } F_{em} \\ v_{dem}(t) - v_a(t)) \times K_{met} \in (0, \infty) \text{ for } F_{met} \\ v_{dem}(t) - v_a(t)) \times K_{sds} \in (-\infty, 0) \text{ for } F_{sds} \end{cases} \tag{3}$$

The saturation logic for electric machines f_{sat} is a scaled replica of Yasa 750 R experimental data [23], which will be described in Figure 5 (b). The two-stage gearbox denoted with "i" shifts when the aircraft reaches 12 m/s. This value is set to ensure that the whole taxi cycle is executed in the first gear whereas during a takeoff and a landing, the second gear is engaged:

$$i(t) = \begin{cases} i(t) = i_{taxi} \text{ for } 0 < |v_a| < 12 \\ i(t) = i_{tl} \text{ for } 12 \leq |v_a| \end{cases} \tag{4}$$

The results validation method relies on the law of conservation of energy. Therefore, the total energy in the system shall remain constant:

$$\sum E(t) = E_{em}(t) + E_{sds}(t) + E_{met}(t) + E_d(t) + E_{rr}(t) + KE_{ac}(t) \tag{5}$$

where energy balance of each factor equals:

$$\begin{cases} E_{em}(t) = \int_0^t (T_{em}(t) \omega_{em}(t)) \\ E_{sds}(t) = \int_0^t (F_{sds}(t) v_a(t)) \\ E_{met}(t) = \int_0^t (F_{met}(t) v_a(t)) \\ E_d(t) = \int_0^t (F_d(t) v_a(t)) \\ E_{rr}(t) = \int_0^t (F_{rr}(t) v_a(t)) \\ KE_{ac}(t) = \frac{1}{2} m {v_a}^2(t) \end{cases} \tag{6}$$

The fuel saving exerted during the aided takeoff is derived from the dynamic model by assuming that the amount of force applied by the landing gear drive system is subtracted from the main engines and multiplied by TSFC:

$$FU_{toff} = \int_0^{t_{TOFF}} (F_{em}(t) \times TSFC) \tag{7}$$

This assumption means that the pilots have to derate the thrust level during takeoff however, this is a common practice in the civilian aviation [24]. To estimate how many kg of fuel can be saved, the TSFC metric is used for static conditions and is equal to 8 [25].

2.2. *Initialization Parameters*

The created model consists of many variables that should accurately represent a narrowbody aircraft and therefore, the values for the Airbus A320 are used. An aircraft is subjected to drag during ground operations and the drag coefficient differs depending on multiple environmental and operational factors such as flaps and slats position. Sun et al. [26] developed a stochastic hierarchical model to provide aerodynamic coefficients. They have provided the aerodynamic coefficients that reflect the landing gear and the flaps extension. The empirical C_d value based on trajectory data of an Airbus A320 equals 0.120. Their study assumes that a reference area is a wing surface area, which is equal to 122.4m^2 for an A320 [27].

Besides of drag, the aircraft is subjected to rolling resistance on ground. The experimental data provided by Yager et al. [28] indicated that the coefficient of rolling resistance changes with velocity. They experimentally assessed the rolling resistance of 40x14-19 tires which are dedicated to similar aircraft, a Boeing 737 and captured the values at 3, 51, and 82 m/s which are equal to 0.01, 0.014, and 0.025 respectively. These values were used in Simulink model as the breakpoints and were linearly interpolated for any velocity value between. Table 2 combines the parameters used in the simulation initialization.

Table 2. Dynamic and fuel saving simulation initialization parameters for the narrowbody aircraft.

Dynamic model		Fuel saving model	
Parameter	Value	Parameter	Value
v_a	0-70 m/s (Fig. 3)	t_{PD}	900 s [29, 30]
m_a	61,700 kg [31]	t_{TXO}	126 s - 1584 s [32]
r_w	0.58 m [33]	t_{TXI}	78 s - 870 s [32]
C_d	0.12 [26]	t_{PARR}	180 s [29]
A	122.4 m^2[27]	t_{OLAP}	30 s [34]
ρ	1.2 kg/m^3	t_{ILAP}	30 s [34]
C_{rr}	0.01 at 3 m/s, 0.014 at 51 m/s, 0.025 at 82 m/s [28]	FC_{APU}	2 kg/min [4]
TSFC	8 g/kN-s[25]	FC_{me}	7.7 kg/min [5]
i_{taxi}	14 (Fig. 5c)	FC_{pp}	315 g/t-km [35, 36, 37, 38, 39]
i_{tl}	2.9 (Fig. 5d)	FU_{toff}	approx. 60 kg (Fig. 5e)
		R_{txi}	0.33 [32]
		R_{txo}	0.67 [32]
		s_f	100-5000 km [31]

The dynamic model reflects the angular speed changes which are influenced by the gear ratio and wheel radius. The latter is equal to 0.58 m according to Dunlop Aircraft Tyres [33] who supplies the tyres to an A320.

The flight path distance influences amount of fuel burned in-flight due to weight penalty. ModernAirlines [31] defined the maximum range of an A320 aircraft as 6100 km, however, the linearization of block fuel intensity is accurate only for the flight paths considerably shorter than maximum range as described in Section 6, and consequently, the flight paths from 100 to 5000 km are taken into account in this study.

2.3. *Drive Cycles*

The realistic drive cycles that consist of taxiing, takeoff and landing are needed to improve understanding of the energy transfer during the ground operations, and therefore, the real data was captured for two commercial missions across Europe. In addition, the quasi-realistic model was made for the third mission by merging the taxi cycles captured by Heinrich et al. [16] with takeoff and landing phases from other flights. The recorded data is presented in Figure 3 and is used as the velocity demand in the MATLAB/ Simulink model.

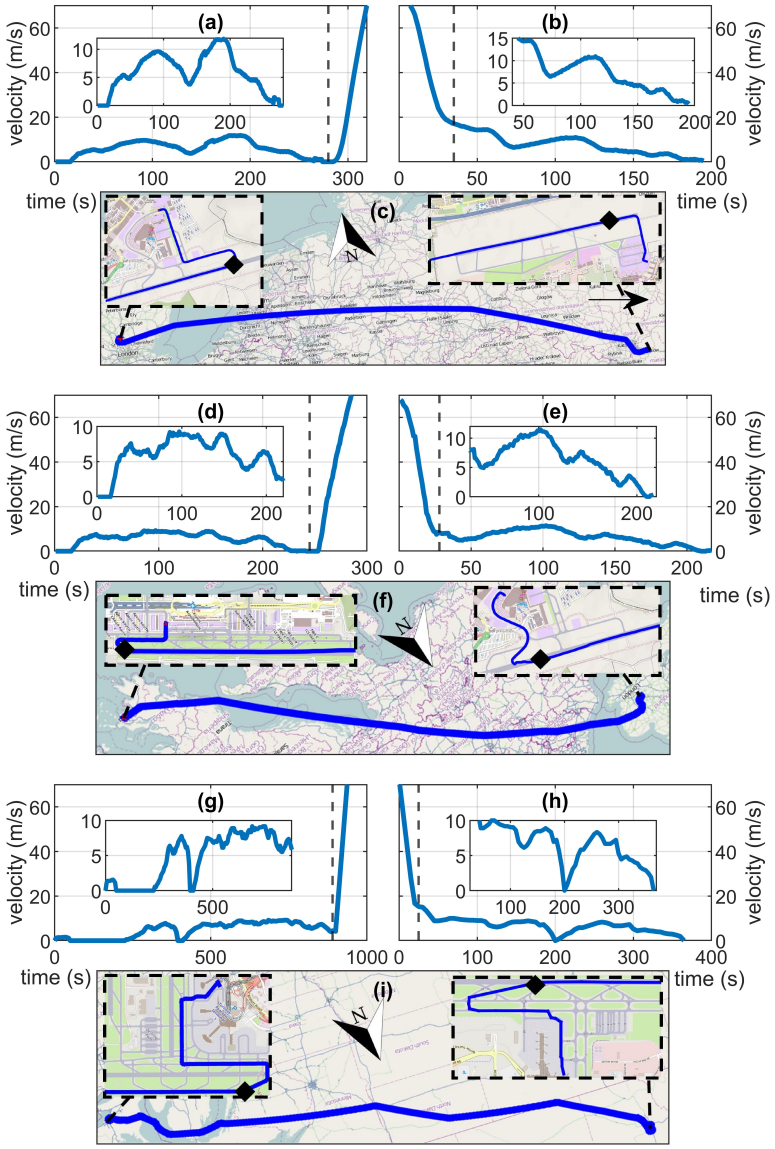

Figure 3. The ground velocity data recorded for two missions ((a) to (f)) and quasi-realistic model for the third ((g) to (i)) . The vertical intermittent lines are the separators for mission phases. Taxi cycles were magnified within each graph: (a) Luton (LTN) taxi-out and takeoff, (b) Krakow (KRK) landing and taxi-in, (c) map for LTN-KRK flight W65002 (d) Athens (ATH) taxi-out and takeoff, (e) Luton (LTN) landing and taxi-in, (f) map for ATH-LTN flight FR7806 (g) Toronto (YYZ) taxi-out and takeoff, (h) Calgary landing and taxi-in, and landing (i) map for YYZ-YYC flight TS682 [16].

The first recorded flight W65002 shown in Figure 3 (a,b,c) took place on 25th of June 2022, from Luton, UK (LTN) to Krakow, PL (KRK) and passed the great circle distance of 1425 km. The taxi-out cycle given in Figure 3 (a) took 280 seconds and was immediately followed by the takeoff. The landing presented in the Figure 3 (b) was followed by taxi-in for approximately three minutes. Figure 3 (d,e,f) presents the flight FR7806 between Athens, Greece (ATH) and Luton that occured on 13th of July 2022. The taxi cycles were comparable in length to the first flight but the flight path was much longer with the great circle distance equal 2450 km. The first flight was executed with the Airbus A321NEO and the second with the B737-800 aircraft, which are designated for mid to long-haul operations but are often used on short flights as well. Each breakpoint consists of longitude, latitude and timestamp where each increment was equal to 1 s. Due to the poor GPS receiver reception, the signal was denoised by applying the moving mean with local 6-point values. Figure 3 (g,h,i) presents the taxiing data captured by Heinrich et al. [16] merged together with takeoff and landing from W65002. This figure is an accurate representation of flight TS682 between Toronto (YYZ) and Calgary (YYC) where the great circle distance is equal to 2700 km. This flight is performed by, among others, the Airbus A320 family aircraft.

3. Electric Power Demand of More Electric Aircraft

The systems of MEA require continuous high power supply and this section explains how much energy the onboard energy storage must provide to allow the all-electric ground operations. The longest mean taxi cycles according to EUROCONTROL [32] are used, where the taxi-out takes 26.3 minutes and the taxi-in occurs for 14.5 minutes. The taxi cycles from Figure 2.3 (g,h) were used in a loop to achieve these longer taxi times. Figure 4 shows power against time for the electric power-consuming systems onboard. The warmup and cooldown cycles of main engines are included in Figure 4 (a,b) and absent in (c,d). The power demand values for all but the landing gear drive system are traced from Section 1 and are taken as an average approximation. The consumption of the landing gear drive system is derived from the dynamic model explained in Section 2.1 and it reflects the recorded taxi cycles.

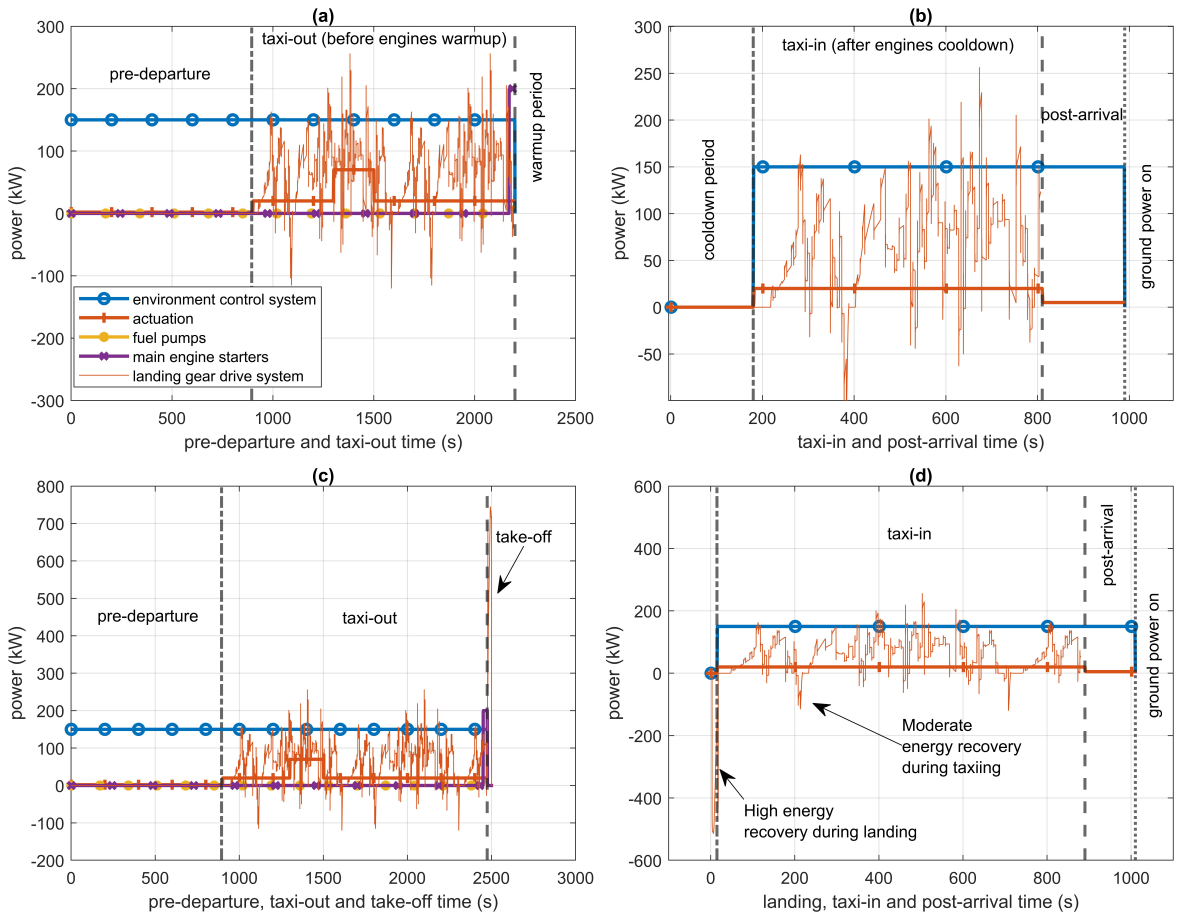

Figure 4. The graphs of power usage against time for the multiple systems during very long ground operations.[9, 10, 11, 32] (a) Longest outbound cycle with respective main engines warmup. (b) Longest inbound with respective main engines cooldown. (c) Longest outbound cycle without warmup (d) Longest inbound cycle without cooldown.

The cycle in each outbound phase shown in Figure 4 (a and c) begins when the ground power is disengaged and electric energy is sourced solely from the battery. In parallel, the ECS is working to provide the air conditioning to the passengers onboard. The average power demand is equal to 150 kW although, this depend on weather conditions and climate zone [11].

More systems start to consume energy as the aircraft begins to move. The electric actuation drains 20 kW and increases for the short period of time when the pilot checks all control surfaces pre-flight. Figure 4 (a) indicates that the highest power demand occurs when the main engines start-up procedure begins. The bleedless main engine starters consume 100 kW each together with the 20kW from fuel pumps. Once running, the main engines supply electrical power to all systems and also charge the battery during the warmup and consequently, analysis stops. Similarly, the power usage during cooldown is neglected in Figure 4 (b). The energy transfer analysis continues up to takeoff and landing phases in Figure 4 (c,d) because these graphs disregard the warmup and the cooldown periods for the main engines. The assumption of neglecting the warmup and cooldown is considered as a potential future technology development which would make energy recovery during landing phase critical. The aircraft requires 194 kWh during the presented ground operations where 48 kWh is used for the landing

gear drive system. The capability of kinetic energy recovery provides over 10 % of required propulsive energy.

4. Landing Gear Drive System Components Sizing and Optimization

The primary aim of the landing gear drive system is to reduce environmental footprint of commercial aviation. Even if the ground operations are completely emission-free, sustainability can be maximized by wisely scaling and optimizing the components to reduce the weight penalty. Accordingly, the system-level sizing and optimization algorithm is proposed and shown in Figure 5 (a). The initial step consists of the power and energy analysis which was accomplished in Section 3. This is followed by the battery size selection that matches the overall energy consumption during the all-electric ground operations. Section 3 explained that the maximum energy needed equals 194 kWh and therefore, the maximum battery capacity needed is rounded to 200 kWh which consists of four modules, 50 kWh each.

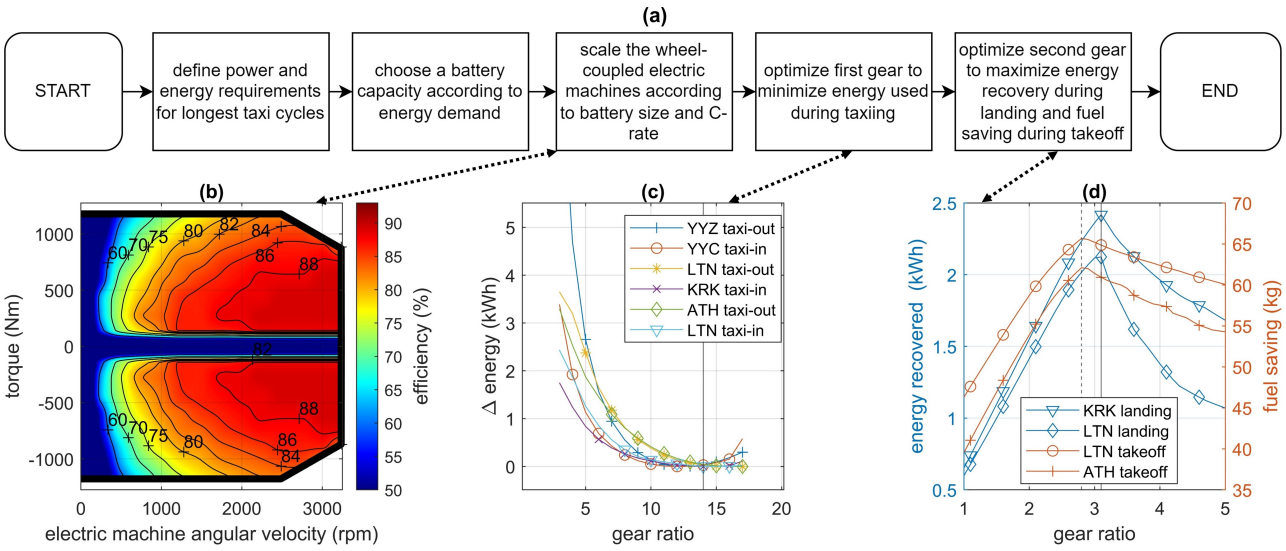

Figure 5. Scaling and optimization of the landing gear drive system. (a) Optimization algorithm, (b) Combined efficiency of electric machines, power converters and drivetrain, (c) gear ratio optimization for taxiing, (d) gear ratio optimization for landing and takeoff.

Once the battery capacity and the maximum C-rate are known, the electric machines, the drivetrain and the power converters are scaled according to the maximum allowable charge rate of the battery leading to 600 kW of total power. Next, the weight for each component is estimated according to the performance metrics disclosed in Table 3. The efficiency rates for the electric machine and the power converter are scaled from the experimental data provided by YASA [23] while the drivetrain is assumed to be 97 % efficient. The total efficiency of the system is demonstrated in Figure 5 (b). The optimization of system performance is done by adjusting the gear ratios of the two-stage gearbox. To optimize taxiing, the taxi cycles from Section 2.3 were extracted and simulated for the multiple gear ratios. Figure 5 (c) shows that gear ratio equal 14 allows to use least energy to propel the aircraft. The second gear was optimized according

to both takeoff fuel saving and landing energy recovery. Figure 2.3 (d) displays the results for both where the optimum ratio is equal to 3.2 for landing and 2.8 for takeoff.

Table 3. System-level performance metrics.

Performance metric of component	2022	2030	2040	2050
Electric machine specific power (kW/kg) [40, 41, 42]	8	16	20	25
4-quadrant power converter specific power (kW/kg) [43]	8.6	13.8	21.1	25.2
Drivetrain specific power (kW/kg) [44, 45, 46, 47, 48]	15	20	25	30
Energy storage specific energy (Wh/kg) [14, 4, 49, 50]	0.25	0.5	0.6	0.7
Energy storage charge rate (C-rate) [4, 18, 19, 15]	3	6	9	N/A

5. Internal Combustion Engines Usage

The fuel combustion during ground operations begins as soon as a pilot turns on the APU at the gate and ends once it is turned off after a ground power unit is connected to the receptacle of aircraft. Ultimately, more phases than the taxiing itself must be taken into account when trying to estimate the fuel burn by aircraft on ground. Figure 6 presents the usage of the onboard ICEs in broader context and includes: (a) pre-departure, (b) taxi-out, (c) landing, (d) taxi-in and (e) post-arrival phases.

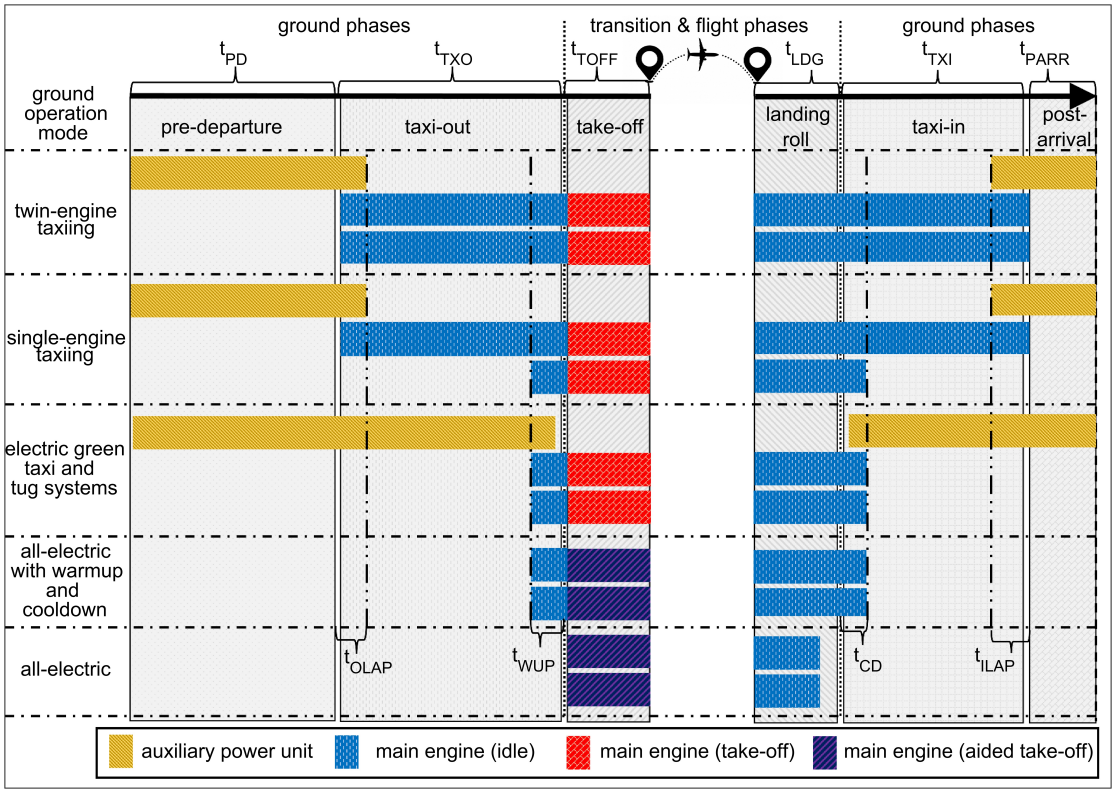

Figure 6. ICE usage during ground and transition phases of mission.

During the pre-departure, the aircraft stands at the gate and the passengers board. The electricity is supplied by the ground power unit while the APU is started as the departure time gets closer. Airport operators limit how much in advance it can be launched and taking Heathrow as an example, the device can be started no earlier than fifteen minutes in advance for a narrow-body aircraft. This time is much greater for large aircraft, an Airbus A380 is allowed to start the APU one hour in advance [29]. There is often a mismatch between regulations and practice, especially when aircraft fly many missions in one day and a delay occurs. Then, the device may be kept on throughout the whole time at the gate. Padhra [30] captured the data for the single day turnarounds around Europe and showed that time between the APU switched on and the aircraft departing is equal to 15 minutes or more for over half of the flights. This is exceptionally important when considering a probability of delay where Zijadić et al. [51] measured that 64 % of arrivals and 46 % of departures were delayed at Sarajevo airport.

The taxi-out phase takes place after the pre-departure and begins with the push-back during which the main engines are started one after another unless operation mode is the single-engine taxiing (SET), thereafter the APU is turned off. There is a small overlap with both types of engines running in parallel and the data recorded by Winther et al. [34] showed that it equals to thirty seconds on average at Copenhagen airport. The timeline is different the for EGTS, where an APU is kept on throughout the taxiing until the main engines have to be started for the warmup procedure, which typically takes three minutes [52]. A similar overlap between the APU and the main engines still occurs with EGTS. The taxi-out ends at the runway and the aircraft begins to takeoff. The main engines are set to higher thrust levels and accordingly consume much more fuel. If present, the landing gear drive system works at full torque to aid the main engines in accelerating the aircraft until 70 m/s is reached.

After arrival, the multiple deceleration systems are engaged during the landing and if weather conditions allow, pilots use the idle thrust reversers. The landing gear drive system also accounts to deceleration and the electric machines work at peak torque rate in the regenerative quadrant leading to kinetic energy being harvested back into the battery.

The fuel consumption throughout the taxiing-in begins with the main engines cooldown period that normally takes three minutes [52]. The procedure begins to differ between the ground operation modes once the main engines can be switched off. One engine is switched off for the SET procedure and both for the electric green taxi systems. If the EGTS is operated, the APU is turned on by the end of cooldown once again with a small overlap that is simulated as thirty seconds.

Once the aircraft arrives at the gate, the main engines are immediately switched off to enable the ground crew to begin their procedures. Then, the APU is disengaged as soon as the ground power is plugged in which takes 3 minutes for 73 % of interday flights [30], whereas the mean time for the Copenhagen airport equals more than four minutes [34]. The maximum period of time for running the APU inbound is regulated by airport operators and Heathrow allows five minutes maximum. We assume that the device is disactivated three minutes after arrival.

6. Net Fuel Savings

The fuel saved during ground operations is reduced by additional fuel burned due to weight penalty in-flight. The weight of the battery is estimated regarding the bat-

tery specific energy $W_{bat} = E_{dem}/SE_{bat}$ and total weight of the electric machines, the power converters and the drivetrain is estimated according to the specific power $W_{pow} = P_{dem}/SP_{em} + P_{dem}/SP_{dr} + P_{dem}/SP_{pcon}$. Finally, the total weight of the system is equal to $W_{tot} = W_{bat} + W_{pow}$.

Once the weight of system is known, we estimate its relation to increased in-flight fuel consumption. This is achieved with the block fuel intensity metric that factors weight of fuel burned per weight of payload per unit of flight distance. Albeit this parameter is highly influenced by aerodynamics and remains nonlinear. Researchers often linearize it which is accurate for flights up to approximately 75 % of maximum aircraft range [35]. Zheng and Rutherford [36] provided the block fuel intensity for the narrowbody aircraft manufactured between 1969 and 2019; the values varied between 200 and 390 grams of fuel per metric tonne-kilometer. These values were compared to Gao et al. [37] experimental aircraft data that comprised fuel usage against payload for the Airbus A321 flights from Beijing (PEK) to Chengdu (CTU) and the Boeing 737 flights from PEK to Shanghai (SZX). The values were between 220-350 for an A321 and between 230-330 for a B737. Yanto and Liem [38] used a slightly different metric of kilograms of fuel per seat-nautical mile. After assuming that a single seat equates to 104 kg of payload [39] the values were equal from 210 to 260. According to gathered data, the conservative value of 315 g per metric tonne-kilometer was used in the simulation.

The block intensity fuel among with the parameters given in Table 2 allow to benchmark the net fuel savings of the landing gear drive system against the other ground movement methods. First, we calculate the fuel consumption exerted by both the APU and the main engines during ground movement :

$$\begin{bmatrix} FU_{ote} \\ FU_{ooe} \\ FU_{oEGTS} \\ FU_{wup} \end{bmatrix} = \begin{bmatrix} t_{PD} + t_{OLAP} \\ t_{PD} + t_{OLAP} \\ t_{PD} + t_{TXO} - t_{WUP} + t_{OLAP} \\ 0 \end{bmatrix} \cdot FC_{APU} + \begin{bmatrix} 2 \times t_{TXO} \\ t_{TXO} + t_{WUP} \\ 2 \times t_{WUP} \\ 2 \times t_{WUP} \end{bmatrix} \cdot FC_{me} \quad (8)$$

Similarly, the fuel consumption for the inbound ground operations is equal to:

$$\begin{bmatrix} FU_{ite} \\ FU_{ioe} \\ FU_{iEGTS} \\ FU_{cd} \end{bmatrix} = \begin{bmatrix} t_{PAR} + t_{ILAP} \\ t_{PAR} + t_{ILAP} \\ t_{PAR} + t_{TXI} - t_{CD} + t_{ILAP} \\ 0 \end{bmatrix} \cdot FC_{APU} + \begin{bmatrix} 2 \times t_{TXI} \\ t_{TXI} + t_{CD} \\ 2 \times t_{CD} \\ 2 \times t_{CD} \end{bmatrix} \cdot FC_{me} \quad (9)$$

The division between outbound and inbound ground fuel consumption is important for the incurred weight penalty. If the landing gear drive system saves fuel during inbound ground operations, the mass of saved fuel can be subtracted from the total weight penalty of the system. The incurred fuel burn due to weight penalty is calculated:

$$\begin{bmatrix} FP_{te} \\ FP_{oe} \\ FP_{EGTS} \end{bmatrix} = \begin{bmatrix} W_{tot} - W_{APU} - FU_{ite} + FU_{cd} \\ W_{tot} - W_{APU} - FU_{ioe} + FU_{cd} \\ W_{tot} - W_{APU} - W_{EGTS} - FU_{iEGTS} + FU_{cd} \end{bmatrix} \cdot S_f \cdot FC_{pp} \quad (10)$$

Once the fuel consumption during the ground operations and the additional fuel burn due to weight penalty are known, the estimation of fuel saving is done:

$$\begin{bmatrix} \mathrm{FS_{te}} \\ \mathrm{FS_{oe}} \\ \mathrm{FS_{EGTS}} \end{bmatrix} = \begin{bmatrix} \mathrm{FU_{ote}} \\ \mathrm{FU_{ooe}} \\ \mathrm{FU_{oEGTS}} \end{bmatrix} + \begin{bmatrix} \mathrm{FU_{ite}} \\ \mathrm{FU_{ioe}} \\ \mathrm{FU_{iEGTS}} \end{bmatrix} - \begin{bmatrix} \mathrm{FP_{te}} \\ \mathrm{FP_{oe}} \\ \mathrm{FP_{EGTS}} \end{bmatrix} + \begin{bmatrix} \mathrm{FU_{toff}} - \mathrm{FU_{wup}} - \mathrm{FU_{cd}} \\ \mathrm{FU_{toff}} - \mathrm{FU_{wup}} - \mathrm{FU_{cd}} \\ \mathrm{FU_{toff}} - \mathrm{FU_{wup}} - \mathrm{FU_{cd}} \end{bmatrix} \tag{11}$$

Some flights at smaller airports have shorter taxiing times than the required warmup and cooldown periods. Consequently, an aircraft will turn on the main engines at the gate and such a special case is considered in the calculus by assuming that the t_{TXO} equals t_{WUP} and T_{PD} is corrected with the initial difference between t_{TXO} and t_{WUP}. The similar logic is applied to inbound ground movement if the t_{CD} exceeds t_{TXI}. The presented equations also allow to neglect completely the warmup and cooldown cycles. In these circumstances, FU_{wup}, FU_{cd}, t_{WUP} and t_{CD} are equal to zero.

The recorded ground movement data from Figure 2.3 is now used to estimate the fuel savings for each flight. Table 4 presents the expected fuel savings for the system with modular battery packs.

Table 4. Simulation results for the ground movement data of three different missions

Flight	Luton-Krakow W65002 Fig.3(a,b,c)	Athens-Luton FR7806 Fig. 3(d,e,f)	Toronto-Calgary TS682 Fig. 3(g,h,i)
Energy storage capacity (kWh)	50 (1 module)	50 (1 module)	100 (2 modules)
Fuel savings against twin-engine taxiing (kg)	103	81	328
Fuel savings against single-engine taxiing (kg)	78	53	102
Fuel savings against electric green taxiing system (kg)	234	335	247

The results show that each mission augmented with the landing gear drive system has the improved fuel economy. The greatest savings are calculated against the EGTS because the weight penalty with modular batteries is lower than the weight penalty of the EGTS which also requires the APU. Therefore, economy is improved during both ground movement and in-flight.

7. Parametric Study for Fuel Savings

Each aircraft mission is unique when considering duration of mission phases. In this section, the landing gear drive system is simulated with respect to varying flight distance and cumulative taxiing time. Different taxiing duration is considered although, the post-departure and the post-arrival time remains constant at 15 and 3 minutes respectively. The cumulative taxi times are distributed with respect to the proportion between taxi-out and taxi-in times derived from the mean taxi duration for 555 airports provided by EUROCONTROL [32] and equal two-third and one-third respectively. Figure 7 presents the parametric study results for an Airbus A320 which

performs the standardized missions with varying cumulative taxi times and flight path lengths.

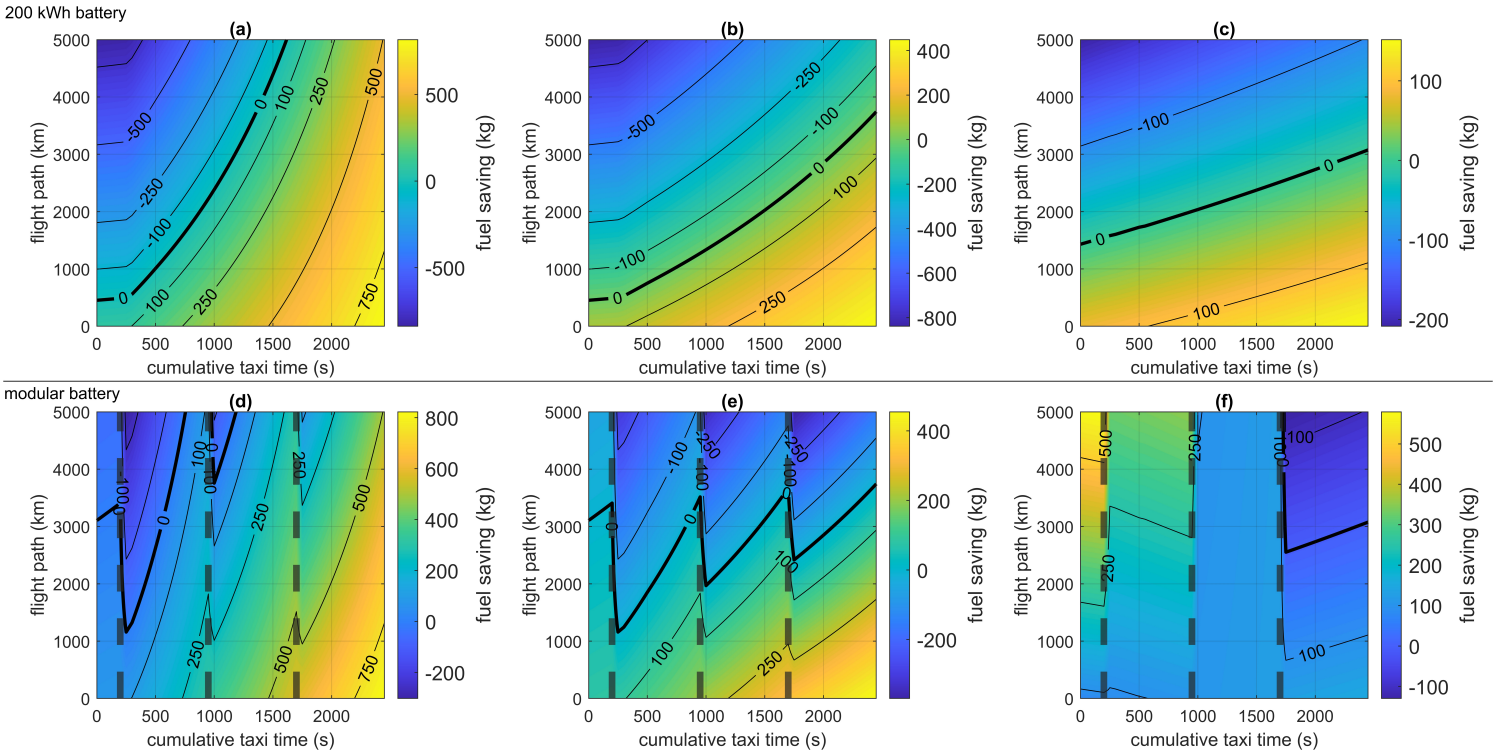

Figure 7. Fuel saving simulation results for technology level from 2022. Negative values indicate the excessive fuel consumed due to weight penalty. The first row assumes that all battery modules are present whereas the second row reflects the module removal for shorter taxiing cycles (indicated by the dashed lines) . The landing gear drive system was benchmarked with: (a,d) Twin-engine taxiing (TET), (b,e) Single-engine taxiing (SET) , (c,f) EGTS and tugs.

During short-haul flights, the landing gear drive system provides the net fuel savings against each conventional ground operation mode. The greatest fuel savings are achieved in Figure 7 (a,d) where TET operation mode was replaced. Depending on the cumulative taxi time, the system can be advantageous for all simulated flight distances including the medium-haul flights. The net savings are lower in Figure 7 (b,e), which shows the comparison with the single-engine taxiing. Nevertheless, the system remains advantageous for flights up to 3000 km during longer taxiing times. Figure 7(c,f) depicts net fuel saving against the EGTS. Albeit the lower peak savings are indicated, the results are more consistent across all cumulative taxiing times. The savings are expected for every flight up to 1200 km, which is the case for nearly every domestic flight. Finally, the results from Figure 7 (d,e,f) show that modular batteries maximize the net fuel savings where the intermittent lines indicate that the additional 50 kWh battery modules are inserted when cumulative taxiing time exceeds 200 s, 950 s and 1700 s. Furthermore, the benchmark with the EGTS in Figure 7 (f) shows the negative slope when the first and the second module are present. This is caused by smaller weight penalty incurred by the landing gear driving system than by the EGTS.

The fuel saving is accrued at the price of electricity needed to charge the battery. Heathrow Airport Ltd. [53] meters the ground unit electricity supply and charges 19 pence per kWh. For the full, 200 kWh charge of the system at 90 % charging efficiency

it would cost £42. This cost is offset by the fuel saving reaching as much as 500 kg. The assumption of 250 kg fuel saving which costs £1.71 per kg [54] yields £373 saving per flight and corresponds to 7 % of a total fuel price reduction for a flight from London Heathrow to Glasgow [55].

8. Landing Gear Drive System in Future

Any novel aircraft system implementation is more likely to succeed during the conceptual stage of aircraft development rather than during retrofitting to the air vehicles already in service. Retrospectively, the Airbus A350 programme was launched in 2005 while the aircraft entered service ten years later and similarly, eight years elapsed between announcement of Boeing 787 and its entering into service in 2011 [56]. In parallel, the electric vehicle components were significantly improved. Energy storage is a textbook example because the specific energy of battery cells available for aviation nearly doubled in last decade [14] and this performance metric will unquestionably improve in the coming years. Accordingly, commercial aircraft concepts that are being discussed at present should include the landing gear drive system with performance metrics that will be available in near future.

The predicted increase in number of commercial aircraft in service will inevitably lead to increased taxi times unless the airport operational efficiency is increased by, for example, the fully autonomous taxiing. In the automotive industry, reduced congestions and traffic flow improvement are highlighted when describing autonomous cars [57] and the same conclusion is drawn for the fully automated taxiing of aircraft [8]. The landing gear drive system is a large step towards the autonomous taxiing for multiple reasons. Primarily, the operation of the electric taxiing system is much simpler when compared to the main engines. Turbofans and turboprops are very complex and pilots have to spend considerable amount of time following the checklists to ensure a safe operation whereas electric machines would require much less attention. Accordingly, the autonomous operation algorithm would be simplified as well. Another factor that currently hinders the autonomous taxiing idea is the jet blast which is a serious threat for airports and ground crew. Implementation of the landing gear drive system allows to keep the main engines off until an aircraft reaches a runway. Similarly, the risk of FOD would be inapplicable because the aircraft would be solely propelled by the wheel drive. Finally, the high-power landing gear drive system offers better controlability because the torque response would be nearly instant when compared to the main engines which take time to spool up and provide thrust.

The energy storage accounts for more than half of the total weight in the landing gear drive system, however, the upcoming technologies potentially allow to reduce or completely remove the weight penalty incurred by the proposed system. This can be achieved by combining the wheel drive with a large energy storage already available onboard of future aircraft. Xie et al. [58] reviewed the hybrid electric powered aircraft concept that incorporates large batteries. They estimated as much as 30 % fuel economy improvement with the hybrid technology. A further step is an all-electric aircraft which receives increasing attention. This concept assumes that the ICEs are absent onboard, and the propulsive power is generated with electric machines only. Currently, the low specific energy of batteries is a restraining factor for this technology [59, 60, 61]. The landing gear drive system would potentially reduce severity of poor battery performance by increasing the energy efficiency of all-electric aircraft during ground movement. The energy transfer benchmark between the propeller- and the

wheel-driven taxiing would provide the answer about feasibility.

Battery technology has seen significant improvement such as fast charging, high efficiency and lightweight designs. Furthermore, the current research areas include structural batteries which are also known as the massless energy storage [62]. They aim to significantly reduce the weight of battery-powered vehicles by integrating the battery into the structure and consequently, the requirement for a separate battery is reduced or eliminated.

The discussed advantages of future technology are combined in Figure 8, which demonstrates the projected increase in the net fuel savings of the landing gear drive system.

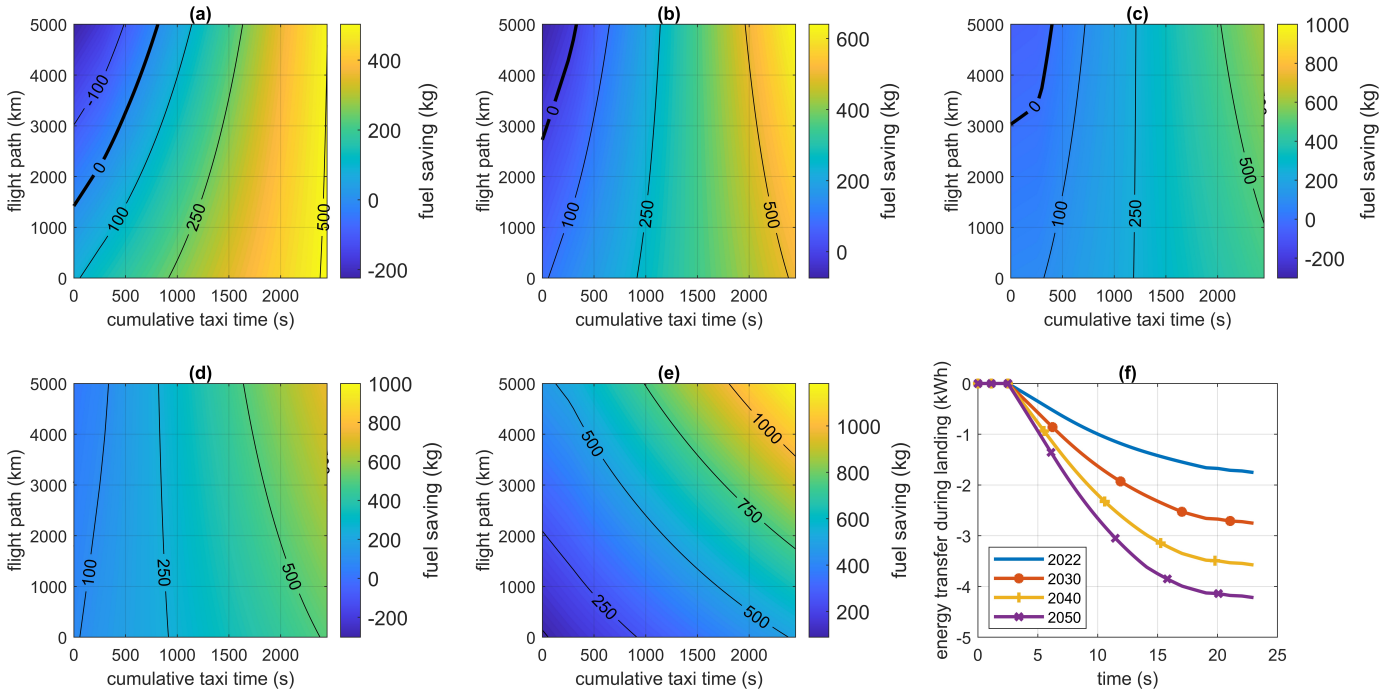

Figure 8. Simulation results of fuel and energy saving for future technology. Negative values indicate the excessive fuel consumed due to weight penalty. (a) 2030 performance metrics against single-engine taxiing (SET), (b) 2040 performance metrics against SET, (c) 2050 performance metrics against SET, (d) 2050 performance metrics combined with the neglected warmup and cooldown cycles against SET, (e) 2050 performance metrics combined with the battery weight, warmup and cooldown cycles neglected. (f) Energy recovery during W65002 landing for present and future performance metrics.

The system-level improvements will primarily impact the weight penalty. The benchmark in Figure 8 (a,b,c) is made with an assumption that the battery capacity and the power of the system remains unchanged but the improved performance shown in Table 3 allows weight reduction. Figure 8 (a) shows that the net fuel savings against the SET will exceed 500 kg in 2030 and the growth will continue to 2040 (see Fig. 8 b), while there is a stagnation towards 2050 as depicted in Figure 8 (c). This lack of improvement is caused by the warmup and cooldown periods of main engines during which jet fuel is consumed. The future technology may allow to skip these cycles and Figure 8 (d) depicts the fuel savings of 2050 technology level with the warmup and cooldown cycles neglected. Further weight reduction can be achieved by considering an MEA with the large energy storage already fitted onboard. Thus, the battery weight can be ignored when calculating the weight penalty of the landing gear drive

system, and Figure 8 (e) indicates that the net fuel savings would exceed 1000 kg for the longest flights. The slope shows that the amount of fuel saved increases also with flight distance. In other words, the weight penalty without battery will be lower than the mass of fuel needed for inbound ground operations in 2050.

Instead of reduced weight, the design objective may be set to maximize harvested energy during landing. Therefore, weight of the system in future would remain constant with the mechanical power increased. Figure 8 (f) shows the amount of energy recovered by the landing gear drive system during the W65002 landing for different technology levels. In 2050, the 1600 kW electric machines would be capable of harvesting over 4 kWh which corresponds to about 16 % of dissipated energy during landing by all deceleration systems fitted onboard.

9. Conclusions

The call for electrification of aviation was addressed in this paper with a landing gear drive system for short-haul MEA. The present work introduced the novel landing gear drive system that combines the multiple academic developments and introduced the regenerative braking during landing to maximize energy efficiency of operation. Therefore, the primary obstacle for electrified aircraft, namely the specific energy of battery, was overcame to the extent that the system was proved to be both sustainably and economically feasible.

The landing gear drive system depleted approximately a quarter of the energy storage capacity during taxiing while the rest was used by the ECS, actuation, fuel pumps and main engine starters. The battery present onboard consisted of 50 kWh modules that stacked up to 200 kWh. This much of energy allowed an Airbus A320 to execute the all-electric taxi cycles as long as 26 minutes. To maximize the energy efficiency, the kinetic energy recovery was added during the landing and it allowed to harvest approximately 10% of available energy. The anticipated quantity of the fuel savings depended on flight distance and taxiing time. The calculation according to the present fuel and electricity prices demonstrated considerable cost reduction of short-haul flights with 7 % of a total fuel price reduction for a flight from London Heathrow to Glasgow. The fuel saving projections were also made according to the future performance metrics and in 2050, the landing gear drive system would reduce the overall consumption for nearly every mission For the best cases, more than 500 kg of fuel would be saved.

The presence of the large battery fitted onboard will further accelerate the electrification of the aerospace industry because it can be shared in-flight with multiple systems such as the hybrid-electric propulsion. Consequently, researchers and aircraft manufacturers will be able to work on concepts that were otherwise inapplicable due to limited specific energy of batteries. In distant future, it is likely that the industry will move away from fossil fuels and therefore, the future work should focus on the landing gear drive system feasibility for all-electric aircraft.

10. Data Availability Statement

The data that support the findings of this study are openly available in Cranfield Online Research Data (CORD) at https://doi.org/10.17862/cranfield.rd.22013231.v1 .

11. Acknowledgments

The authors acknowledge the support received from the EPSRC [Grant Number 2517982] and Airbus Operations Ltd. For the purpose of open access, the author has applied a Creative Commons Attribution (CC BY) licence to any Author Accepted Manuscript version arising.

References

[1] S. Shparberg and B. Lange, "Global Market Forecast 2022," Airbus, Touluse, Tech. Rep., 2022.

[2] European Union Aviation Safety Agency, *European aviation environmental : report 2019.* Publications Office, 2019.

[3] P. Giangrande, A. Galassini, S. Papadopoulos, A. Al-Timimy, G. L. Calzo, M. Degano, M. Galea, and C. Gerada, "Considerations on the Development of an Electric Drive for a Secondary Flight Control Electromechanical Actuator," *IEEE Transactions on Industry Applications*, vol. 55, no. 4, pp. 3544–3554, jul 2019. [Online]. Available: https://doi.org/10.1109/TIA.2019.2907231

[4] A. A. Recalde, G. Student Member, M. Lukic, A. Hebala, P. Giangrande, S. Member, C. Klumpner, S. Nuzzo, P. H. Connor, J. A. Atkin, S. V. Bozhko, and M. Galea, "Energy Storage System Selection for Optimal Fuel Consumption of Aircraft Hybrid Electric Taxiing Systems," *IEEE TRANSACTIONS ON TRANSPORTATION ELECTRIFICATION*, vol. 7, no. 3, 2021. [Online]. Available: https://doi.org/10.1109/TTE.2020.3039759

[5] H. J. Kim and H. Baik, "Empirical Method for Estimating Aircraft Fuel Consumption in Ground Operations," vol. 2674, no. 12, pp. 385–394, oct 2020. [Online]. Available: https://doi.org/10.1177/0361198120961033

[6] SAE International, "Landing Gear (Engine Off) Taxi System AIR6246," 2021.

[7] D. Rohacs and J. Rohacs, "Magnetic levitation assisted aircraft take-off and landing (feasibility study – GABRIEL concept)," *Progress in Aerospace Sciences*, vol. 85, pp. 33–50, 2016. [Online]. Available: http://dx.doi.org/10.1016/j.paerosci.2016.06.001

[8] M. Lukic, P. Giangrande, A. Hebala, S. Nuzzo, and M. Galea, "Review, Challenges, and Future Developments of Electric Taxiing Systems," *IEEE Transactions on Transportation Electrification*, vol. 5, no. 4, pp. 1441–1457, dec 2019. [Online]. Available: https://doi.org/10.1109/TTE.2019.2956862

[9] M. Pagonis, "Electrical power aspects of distributed propulsion systems in turbo-electric powered aircraft," Ph.D. dissertation, Cranfield University, 2015. [Online]. Available: http://dspace.lib.cranfield.ac.uk/handle/1826/9873

[10] P. W. Wheeler, J. C. Clare, A. Trentin, and S. Bozhko, "An overview of the more electrical aircraft." [Online]. Available: https://doi.org/10.1177/0954410012468538

[11] J. Herzog, "Electrification of the environmental control system," in *25th International congress of the aeronautical sciences*, vol. 3, 2006, pp. 2006–2008.

[12] J. A. Stockford, C. Lawson, and Z. Liu, "Benefit and performance impact analysis of using hydrogen fuel cell powered e-taxi system on A320 class airliner," *The Aeronautical Journal*, vol. 123, no. 1261, pp. 378–397, mar 2019. [Online]. Available: https://doi.org/10.1017/aer.2018.156

[13] Z. Wang, D. Ouyang, M. Chen, X. Wang, Z. Zhang, and J. Wang, "Fire behavior

of lithium-ion battery with different states of charge induced by high incident heat fluxes," *Journal of Thermal Analysis and Calorimetry*, vol. 136. [Online]. Available: https://doi.org/10.1007/s10973-018-7899-y

[14] V. Viswanathan, A. H. Epstein, Y.-M. Chiang, E. Takeuchi, M. Bradley, J. Langford, and M. Winter, "The challenges and opportunities of battery-powered flight," *Nature*, vol. 601, p. 519, 2022. [Online]. Available: https://doi.org/10.1038/s41586-021-04139-1

[15] T. R. Tanim, E. J. Dufek, M. Evans, C. Dickerson, A. N. Jansen, B. J. Polzin, A. R. Dunlop, S. E. Trask, R. Jackman, I. Bloom, Z. Yang, and E. Lee, "Extreme Fast Charge Challenges for Lithium-Ion Battery: Variability and Positive Electrode Issues," *Journal of The Electrochemical Society*, vol. 166, no. 10, pp. A1926–A1938, jun 2019. [Online]. Available: https://doi.org/10.1149/2.0731910jes

[16] M. T. E. Heinrich, F. Kelch, P. Magne, and A. Emadi, "Regenerative Braking Capability Analysis of an Electric Taxiing System for a Single Aisle Midsize Aircraft," *IEEE TRANSACTIONS ON TRANSPORTATION ELECTRIFICATION*, vol. 1, no. 3, 2015. [Online]. Available: https://doi.org/10.1109/TTE.2015.2464871

[17] J. Deja, I. Dayyani, and M. Skote, "Modeling and performance evaluation of sustainable arresting gear energy recovery system for commercial aircraft," *International Journal of Green Energy*, pp. 1–15, nov 2022. [Online]. Available: https://doi.org/10.1080/15435075.2022.2143715

[18] W. Xie, X. Liu, R. He, Y. Li, X. Gao, X. Li, Z. Peng, S. Feng, X. Feng, and S. Yang, "Challenges and opportunities toward fast-charging of lithium-ion batteries," 2020. [Online]. Available: https://doi.org/10.1016/j.est.2020.101837

[19] L.-L. Lu, Y.-Y. Lu, Z.-X. Zhu, J.-X. Shao, H.-B. Yao, S. Wang, T.-W. Zhang, Y. Ni, X.-X. Wang, and S.-H. Yu, "Extremely fast-charging lithium ion battery enabled by dual-gradient structure design," *Sci. Adv*, vol. 8, p. 6624, 2022. [Online]. Available: https://doi.org/10.1126/sciadv.abm6624

[20] D. Scholz, "An optional APU for passenger aircraft," in *5th Council of European Aerospace Societies Air and Space Conference: Challenges in European Aerospace, Delft*, 2015.

[21] S. Dunn, "Master Minimum Equipment List (MMEL) Boeing 737 MAX," Des Moines, 2020.

[22] T. F. Johnson, "Electric green taxiing system (EGTS) for aircraft," *IEEE Transactions on Transportation Electrification Web Portal*, 2016.

[23] YASA, "Yasa 750 R," 2022. [Online]. Available: https://www.yasa.com/products/yasa-750/

[24] L. Sherry and S. Neyshabouri, "Estimating takeoff thrust from surveillance track data," in *Transportation Research Board Annual Meeting*, 2014.

[25] A. Bensel, *Characteristics of the Specific Fuel Consumption for Jet Engines*. Hamburg: Aircraft Design and Systems Group (AERO), Department of Automotive . . . , 2018.

[26] J. Sun, J. M. Hoekstra, and J. Ellerbroek, "Estimating aircraft drag polar using open flight surveillance data and a stochastic total energy model," *Transportation Research Part C: Emerging Technologies*, vol. 114, pp. 391–404, may 2020. [Online]. Available: https://doi.org/10.1016/j.trc.2020.01.026

[27] L. Jenkinson, P. Simpkin, and D. Rhodes, "Civil Jet Aircraft Design," *Civil Jet Aircraft Design*, jan 1999. [Online]. Available: https://booksite.elsevier.com/9780340741528/appendices/data-a/default.htm

[28] T. J. Yager, S. M. Stubbs, and P. A. Davis, "Aircraft Radial-Belted Tire Evaluation," *SAE Transactions*, vol. 99, pp. 1752–1759, may 1990. [Online]. Available: http://www.jstor.org/stable/44473143

[29] Environmental Management: Heathrow Airport, "Operational Safety Instruction - Use of Aircraft Auxiliary Power Units," 2018. [Online]. Available: https://www.heathrow.com/content/dam/heathrow/web/common/documents/company/team-heathrow/airside/operational-safety-insttructions/ASEnv_OSI_078.pdf

[30] A. Padhra, "Emissions from auxiliary power units and ground power units during intraday aircraft turnarounds at European airports," *Transportation Research Part D: Transport and Environment*, vol. 63, pp. 433–444, aug 2018. [Online]. Available: https://doi.org/10.1016/J.TRD.2018.06.015

[31] ModernAirlines, "ModernAirliners," 2021. [Online]. Available: https://modernairliners.com/

[32] EUROCONTROL, "Taxi Times - Summer 2021," 2022. [Online]. Available: https://www.eurocontrol.int/publication/taxi-times-summer-2021

[33] Dunlop Aircraft Tyres, "DR15348T Specification," 2022. [Online]. Available: https://www.dunlopaircrafttyres.co.uk/tyres/detail/dr15348t

[34] M. Winther, U. Kousgaard, T. Ellermann, A. Massling, J. K. Nøjgaard, and M. Ketzel, "Emissions of NO x , particle mass and particle numbers from aircraft main engines, APU's and handling equipment at Copenhagen Airport," *Atmospheric Environment*, vol. 100, pp. 218–229, jan 2015. [Online]. Available: https://doi.org/10.1016/j.atmosenv.2014.10.045

[35] M. Burzlaff, *Aircraft Fuel Consumption-Estimation and Visualization*. Aircraft Design and Systems Group (AERO), Department of Automotive and . . . , 2017.

[36] X. Zheng and D. Rutherford, "Fuel burn of new commercial jet aircraft: 1960 to 2019," 2020.

[37] Y.-Q. Gao, T.-Q. Tang, J. Zhang, and F. You, "Which aircraft has a better fuel efficiency? – a case study in china," *Transportmetrica B: Transport Dynamics*, vol. 10, no. 1, pp. 1032–1045, Dec 2022. [Online]. Available: https://doi.org/10.1080/21680566.2021.1997674

[38] J. Yanto and R. P. Liem, "Aircraft fuel burn performance study: A data-enhanced modeling approach," *Transportation Research Part D: Transport and Environment*, vol. 65, pp. 574–595, 2018. [Online]. Available: https://doi.org/10.1016/j.trd.2018.09.014

[39] Z. Berdowski, J. T. van den Broek-Serie, Y. K. Jetten, and Y. Kawabata, "Survey on standard weights of passengers and baggage," *European Aviation Safety Agency, Cologne, Germany*, 2009.

[40] C. L. Pastra, C. Hall, G. Cinar, J. Gladin, and D. N. Mavris, "Specific Power and Efficiency Projections of Electric Machines and Circuit Protection Exploration for Aircraft Applications," in *2022 IEEE Transportation Electrification Conference Expo (ITEC)*. IEEE, jun 2022, pp. 766–771. [Online]. Available: https://doi.org/10.1109/ITEC53557.2022.9813927

[41] X. Zhang, C. L. Bowman, T. C. O'Connell, and K. S. Haran, "Large electric machines for aircraft electric propulsion," *IET Electric Power Applications*, vol. 12, no. 6, pp. 767–779, jul 2018. [Online]. Available: https://doi.org/10.1049/IET-EPA.2017.0639

[42] J. Z. Bird, "A Review of Electric Aircraft Drivetrain Motor Technology," *IEEE TRANSACTIONS ON MAGNETICS*, vol. 58, no. 2, p. 8201108, 2022. [Online]. Available: https://doi.org/10.1109/TMAG.2021.3081719.

[43] C. Hall, C. L. Pastra, A. Burrell, J. Gladin, and D. N. Mavris, "Projecting Power Converter Specific Power Through 2050 for Aerospace Applications," in *2022 IEEE Transportation Electrification Conference Expo (ITEC)*. IEEE, jun 2022, pp. 760–765. [Online]. Available: https://doi.org/10.1109/ITEC53557.2022.9813991

[44] F1Chronicle, "How Much Horsepower does an F1 Car Have?" [Online]. Available: https://f1chronicle.com/how-much-horsepower-does-an-f1-car-have/#:$\sim$:text=AccordingtotheSCAexpert,speedsaround400km%2Fh.

[45] L. Rimmer, "How Much Does an F1 Car Weigh?" 2022. [Online]. Available: https://www.autosport.com/f1/news/how-much-does-an-f1-car-weigh/10246442/

[46] XTRAC, "P1227 Integrated Lightweight Electric Vehicle (ILEV) Transmission," 2022. [Online]. Available: https://www.xtrac.com/product/p1227-integrated-lightweight-electric-vehicle-ilev-transmission/

[47] P. Maric, "Porsche Taycan: A look at its motors, transmission, and dynamic chassis," 2019. [Online]. Available: https://www.drive.com.au/news/porsche-taycan-a-look-at-its-motors-transmission-and-dynamic-chassis/

[48] P. Liu and S. Feng, "Integrated Motor and Two-speed Gearbox Powertrain System Development for Electric Vehicle," in *2020 IEEE Energy Conversion Congress and Exposition (ECCE)*. IEEE, oct 2020, pp. 1499–1504. [Online]. Available: https://doi.org/10.1109/ECCE44975.2020.9236397

[49] M. Pagliaro, F. Meneguzzo, W. Shi, T. Stedman, and L. M. Woods, "The driving power of the electron," *J. Phys.: Energy*, vol. 1, p. 11001, 2019. [Online]. Available: https://doi.org/10.1088/2515-7655/aacd9f

[50] J. Serafini, M. Cremaschini, G. Bernardini, L. Solero, C. Ficuciello, and M. Gennaretti, "Conceptual All-Electric Retrofit of Helicopters: Review, Technological Outlook, and a Sample Design," *IEEE Transactions on Transportation Electrification*, vol. 5, no. 3, pp. 782–794, 2019. [Online]. Available: http://doi.org/10.1109/TTE.2019.2919893

[51] N. Zijadić, E. Ganić, M. Bračić, and I. Štimac, "Impact of Aircraft Delays on Population Noise Exposure in Airports Surroundings," *International Journal of Environmental Research and Public Health*, vol. 19, no. 15, p. 8921, jul 2022. [Online]. Available: https://doi.org/10.3390/ijerph19158921

[52] M. R. van Holsteijn, A. Gangoli Rao, and F. Yin, "Operating Characteristics of an Electrically Assisted Turbofan Engine," in *Volume 1: Aircraft Engine; Fans and Blowers*, vol. 1. American Society of Mechanical Engineers, sep 2020, pp. 1–10. [Online]. Available: https://doi.org/10.1115/GT2020-15355

[53] Heathrow Airport Ltd., "Tariffs with effect from 1 January 2022," 2021. [Online]. Available: https://www.heathrow.com/content/dam/heathrow/web/common/documents/company/doing-business-with-heathrow/regulated-charges/General_Notice_01_22_Tariffs_with_effect_from_1_January_2022.pdf

[54] FarNorthAviation, "Latest Aviation Fuel Prices," 2022. [Online]. Available: https://www.farnorthaviation.co.uk/latest-aviation-fuel-prices.html

[55] ICAO, "ICAO Carbon Emissions Calculator," 2022. [Online]. Available: https://www.icao.int/environmental-protection/Carbonoffset/Pages/default.aspx

[56] A. Jiménez-Crisóstomo, L. Rubio-Andrada, M. S. Celemín-Pedroche, and M. Escat-Cortés, "The Constrained Air Transport Energy Paradigm in 2021," 2021. [Online]. Available: https://doi.org/10.3390/su13052830

[57] F. Raissi, S. Yangui, and F. Camps, "Autonomous Cars, 5G Mobile Networks and Smart Cities: Beyond the Hype," in *2019 IEEE 28th International Conference on Enabling Technologies: Infrastructure for Collaborative Enterprises*

(WETICE). IEEE, jun 2019, pp. 180–185. [Online]. Available: https://doi.org/10.1109/WETICE.2019.00046

[58] Y. Xie, A. Savvarisal, A. Tsourdos, D. Zhang, and J. Gu, "Review of hybrid electric powered aircraft, its conceptual design and energy management methodologies," *Chinese Journal of Aeronautics*, vol. 34, no. 4, pp. 432–450, apr 2021. [Online]. Available: https://doi.org/10.1016/J.CJA.2020.07.017

[59] A. W. Schäfer, S. R. H. Barrett, K. Doyme, L. M. Dray, A. R. Gnadt, R. Self, A. O'Sullivan, A. P. Synodinos, and A. J. Torija, "Technological, economic and environmental prospects of all-electric aircraft," *Nature Energy*, vol. 4, no. 2, pp. 160–166, feb 2019. [Online]. Available: https://doi.org/10.1038/s41560-018-0294-x

[60] P. Wheeler, "Technology for the more and all electric aircraft of the future," in *2016 IEEE International Conference on Automatica (ICA-ACCA)*. IEEE, oct 2016, pp. 1–5. [Online]. Available: https://doi.org/10.1109/ICA-ACCA.2016.7778519

[61] A. Barzkar and M. Ghassemi, "Electric power systems in more and all electric aircraft: A review," *Ieee Access*, vol. 8, pp. 169 314–169 332, 2020. [Online]. Available: https://doi.org/10.1109/ACCESS.2020.3024168

[62] L. E. Asp, K. Bouton, D. Carlstedt, S. Duan, R. Harnden, W. Johannisson, M. Johansen, M. K. G. Johansson, G. Lindbergh, F. Liu, K. Peuvot, L. M. Schneider, J. Xu, and D. Zenkert, "A Structural Battery and its Multifunctional Performance," *Advanced Energy and Sustainability Research*, vol. 2, no. 3, p. 2000093, mar 2021. [Online]. Available: https://doi.org/10.1002/aesr.202000093

2023-03-28

More electric aircraft conversion to all-electric during ground operations: battery powered landing gear drive system

Deja, Jakub

IEEE

Deja J, Dayyani I, Nair V, Skote M. (2023) More electric aircraft conversion to all-electric during ground operations: battery powered landing gear drive system, IEEE Transactions on Transportation Electrification, Available online 28 March 2023

https://doi.org/10.1109/TTE.2023.3262208